Isotope Exchange for Gas-Phase Acetic Acid and Ethanol at Aqueous Interfaces: A Study of Surface Reactions

Q. Shi, Y. Q. Li, and P. Davidovits*

Chemistry Department, Merkert Chemistry Center, Boston College, Chestnut Hill, Massachusetts 02167-3809

J. T. Jayne, D. R. Worsnop, M. Mozurkewich,† and C. E. Kolb

Center for Aerosol and Cloud Chemistry, Aerodyne Research, Inc., Billerica, Massachusetts 01821-3976

Received: August 26, 1998; In Final Form: January 28, 1999

Isotope exchange for deuterated gas-phase acetic acid and ethanol in contact with water (H_2O) droplets was studied using a droplet train apparatus. In these experiments, the gas-phase species interacts with liquid droplets and the loss of the species is monitored. The loss of the species may be due to the entry of the molecules into the bulk or to a reaction of the species at the gas−liquid interface, in this case isotope exchange. Studies were conducted as a function of pH in the range 0−14, droplet temperature in the range 291−263 K and gas−liquid interaction time in the range 2−15 ms. For deuterated acetic acid the isotope exchange probability with water molecules at the interface is near unity. On the other hand, isotope exchange probability for ethanol with surface water molecules at pH 7 is much smaller, ranging from 0.033 at 263 K to 0.051 at 291 K. Ethanol isotope exchange is both acid and base catalyzed. The exchange probability therefore increases both toward low and high pH and levels off to a plateau at pH 2 and 12, respectively. The maximum value of the isotope exchange probability at the plateau is significantly less than 1. It ranges between 0.14 and 0.18 with no clear trend in temperature. Results are explained in terms of a kinetic model in which it is assumed that the surface-adsorbed ethanol molecules are distributed between two distinct forms: a weakly adsorbed state and a partially solvated state. Only the partially solvated molecules can interact with the near-surface ions in the interior of the liquid. A finite rate of entering the partially solvated state is responsible for the observed plateaus in isotope exchange at high and low pH. Parameters describing the gas uptake and isotope exchange processes are examined using two models to describe the surface species: surface nucleation and Gibbs surface excess.

Introduction

The importance in atmospheric chemistry of reactions at the gas−liquid interface and transport of gaseous species into liquid droplets has motivated development of new techniques specifically designed for the study of such interfacial processes.[1] Work in this area has yielded important new information; however, only the very first steps have been taken toward understanding the ways in which gas-phase molecules accommodate on a liquid surface and react with solute or solvent molecules.[2] Much remains to be understood about the nature of the process. For example, experiments measuring the uptake of soluble species, such as alcohols, by water, consistently yield mass accommodation coefficients significantly smaller than 1, indicating that there is a significant barrier to species uptake. On the other hand, molecular dynamics simulations of ethanol uptake by water[3,4] conclude that the mass accommodation coefficient should be essentially unity. The source of the disagreement between the dynamics simulations and the results of experiments is at this point not evident. It is clear, however, that the computer model does not simulate the appropriate barrier to uptake.

To obtain more information about the nature of kinetics at the gas−liquid interface, we have performed a series of experiments studying D to H isotope exchange at the gas−water interface. Isotope exchange experiments have been an important means for elucidating reaction mechanisms in many areas of chemistry. (See, for example, Rouhi, 1997.[5]) The research group of Nathanson used isotope exchange in molecular beam experiments to study interactions of water and several small organic molecules on highly concentrated sulfuric acid surfaces. In these pioneering studies they were able to observe impulsive, trapping, and desorption scattering processes at the sulfuric acid interface.[6−8] To our knowledge, the present work is the first use of isotope exchange to study reactive interactions at the gas−water interface. In these experiments interactions of deuterated gas-phase acetic acid and ethanol with water (H_2O) droplets were studied using a droplet train apparatus. The ethanol measurements were made as a function of pH, gas−liquid interaction time, and droplet temperature. A more limited set of studies examined the interactions of normal gas-phase ethanol in contact with deuterated water (D_2O).

In previous experimental work surface reactivity as a function of reactant concentration was studied for $ClONO_2$,[9,10] for halogen molecules,[11] and for $ClNO_2$.[12] However, in those studies the measured uptake was totally reactive, that is, determined by reactions at the interface and in the bulk liquid. The current isotope exchange experiments with ethanol provide an opportunity to study gas−liquid interactions under conditions where both mass accommodation and surface reactivity, in the form of acid or base-catalyzed isotope exchange, are involved

† Permanent address: Chemistry Department, York University, Toronto, Ontario M3J 1P3, Canada.

10.1021/jp983525a CCC: $18.00
Published on Web 03/11/1999

in the uptake process. In these experiments it is possible to separate the effects of mass accommodation, solubility, and surface reaction. As a result a more complete picture is obtained of kinetics within the gas−liquid interface.

Modeling Gas−Liquid Interactions

In our droplet train experiments, the gas-phase species interacts with liquid droplets and the loss of the gaseous species is monitored. This loss may be due to mass accommodation, i.e., entry of the molecules into the bulk liquid (and possibly subsequent reactions in the bulk liquid), or to a reaction of the species at the gas−liquid interface. The gas−liquid interactions are also affected by gas-phase diffusion and Henry's law saturation.[13−15] For convenience we will first describe a model that characterizes the uptake of gas-phase ethanol in the absence of D−H exchange at the interface and then describe the modification to account for the interfacial isotope exchange.

A phenomenological description of the entry of gases into liquids is straightforward. First, the gas phase molecule is transported to the liquid surface, usually by gas-phase diffusion. The initial entry of the species into the liquid is governed by the mass accommodation coefficient, α, which is the probability that an atom or molecule striking a liquid surface enters into the bulk liquid phase.

$$\alpha = \frac{\text{no. of molecules entering the liquid phase}}{\text{no. of molecular collisions with the surface}} \quad (1)$$

In the absence of surface reactions, the mass accommodation coefficient determines the maximum flux, J, of gas into a liquid, which is given by

$$J = \frac{n_g \bar{c} \alpha}{4} \quad (2)$$

Here n_g is the density of the trace gas phase and $\bar{c}$ is the trace gas average thermal speed. If reactions occur at the gas−liquid interface (e.g., isotope exchange), then the flux of species disappearing from the gas phase may exceed that given by eq 2.

In a laboratory experiment gas uptake by a liquid is usually limited by gas-phase diffusion and often by solubility constraints as the species in the liquid approaches Henry's law saturation. In the latter process, a fraction of the molecules that enters the liquid evaporates back into the gas phase due to the limited solubility of the species. At equilibrium, the liquid is saturated and the flux of molecules into the liquid is equal to the rate of desorption of these molecules out of the liquid. In experiments subject to these effects, the measured flux into a surface is expressed in terms of a measured uptake coefficient, γ_{meas}, as

$$J = \frac{n_g \bar{c} \gamma_{meas}}{4} \quad (3)$$

Since γ_{meas} represents a convolution of the several physical and chemical processes mentioned above, the experimental challenge is to separate the contributions of these processes to the overall gas uptake. The droplet train apparatus allows direct control of many factors affecting the rate of gas uptake and thereby enables the deconvolution of the uptake into its component processes.[13−15]

The droplet train apparatus provides a technique for accurately controlling the gas−liquid interaction time and for continuously renewing the liquid surface. The droplets in the train are closely spaced (3−12 diameters) and move rapidly. This raises two important questions that have to be addressed in connection with the technique. (1) Does the rapid motion of the droplets through the background gas induce internal stirring or circulation that might alter liquid phase transport of solvated species? (2) What is the nature of gas-phase diffusive transport to the droplets. These issues cannot be treated analytically. However, as will be discussed, a series of detailed experiments have demonstrated that the behavior of droplets within the moving train is surprisingly similar to stationary droplets. First, the good agreement with literature values of the Henry's law coefficient for ethanol (and several other species) measured with the droplet train technique proves that internal stirring is not an issue. (See eq 11 and Figure 6.) Second, as will be shown, gas-phase diffusive transport to a train of droplets has the same functional dependence on the Knudsen number (*Kn*) as to a stationary droplet, except that the droplet diameter in *Kn* must be replaced by twice the diameter of the droplet generating orifice. That is, for a given orifice diameter the effective *Kn* for a train of moving closely spaced droplets depends only on the orifice diameter and not on the diameter of the droplets (which can be altered by changing the frequency of droplet generation).

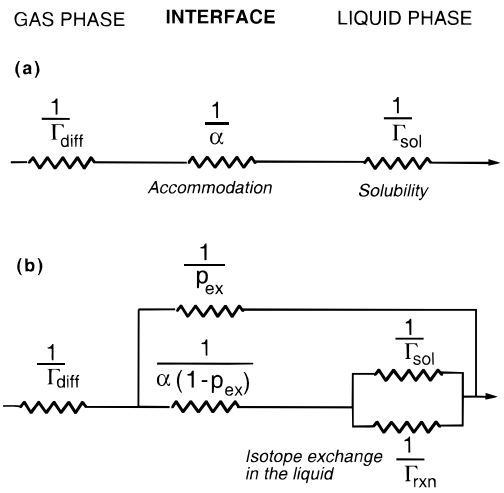

Figure 1. (a) Electrical circuit analogue for the gas uptake process. Terms defined in the text. (b) Electrical circuit analogue for the gas uptake process including surface reactions.

In the absence of D−H exchange, the three processes that affect the uptake of species studied in this work, namely, gas-phase diffusion, mass accommodation, and Henry's law solubility limitation, are coupled to each other and therefore a quantitative description of the uptake process involves coupled differential equations. General solutions for such equations are not available. In special cases, however, the equations can be solved and the processes decoupled. The separated effect of these processes on the gas uptake can be taken into account by dimensionless conductances Γ_{diff}, α, and Γ_{sol}, representing gas-phase diffusion, mass accommodation, and Henry's law solubility, respectively. Expressions for these terms will be presented in the following sections. In the absence of surface reactions, the experimentally measured uptake coefficient γ_{meas} is then expressed as

$$\frac{1}{\gamma_{meas}} = \frac{1}{\Gamma_{diff}} + \frac{1}{\alpha} + \frac{1}{\Gamma_{sol}} \quad (4)$$

An electrical circuit analogue for this representation is shown in Figure 1a.

Mass Accommodation. In accord with the original formulation of Jayne et al.,[16] mass accommodation can be viewed as a

two-step process. First, the gas molecule strikes the surface and is adsorbed as surface species n_s. Adsorption involves thermal accommodation to the surface. In the absence of surface reactions, the surface species then either enters the liquid or desorbs from the surface. The process can be represented as

$$n_g \underset{k_{des}}{\overset{k_{ads}}{\rightleftharpoons}} n_s \xrightarrow{k_{sol}} n_l \tag{5}$$

Here the subscripts g, s, and l represent the gas, surface, and liquid state of the species. In this representation we have omitted the reverse arrow from n_l to n_s because here only the mass accommodation process is represented. The desorption out of the bulk liquid is accounted for separately by Γ_{sol} in eq 4.

The adsorption rate constant (or deposition velocity) is $k_{ads} = S\bar{c}/4$. Here S is the trace gas adsorption coefficient, that is, the fraction of collisions that results in thermal accommodation of the trace gas onto the surface. In the absence of liquid saturation effects (desorption from the liquid), the uptake flux is expressed in terms of the incoming and outgoing fluxes as

$$\alpha n_g \bar{c}/4 = n_g S\bar{c}/4 - n_s k_{des} \tag{6}$$

and by mass conservation

$$\alpha n_g \bar{c}/4 = n_s k_{sol} \tag{7}$$

From these relationships we obtain

$$1/\alpha = 1/S + k_{des}/Sk_{sol} \tag{8}$$

We expect S to be very close to unity with the gas−liquid surface collisions occurring at the speeds associated with the relatively low temperature of our experiments.[2,17] Consequently, we will assume $S = 1$ in the data analysis described below.

Solubility. In this section we derive an expression for Γ_{sol}. We begin with the equilibrium relationships between gas-phase and solvated species concentrations [X(g)] and [X(aq)] as given by the Henry's law coefficient H (M atm^{-1}):

$$X(g) \overset{H}{\rightleftharpoons} X(aq) \tag{R1}$$

The Henry's law coefficient, H, is defined as:

$$[X(aq)] = p_X H = [X(g)]RTH \tag{R2}$$

where R is the gas constant in units of atm M^{-1} K^{-1}. On short time scales of our experiments, the volume of liquid subject to Henry's law saturation is determined by liquid-phase diffusion.

We define $\gamma_o(t)$ as the uptake coefficient in the limit where diffusion of the trace gas to the droplet surface is not rate limiting. Danckwerts[18,19] provides a solution for the uptake coefficient $\gamma_o(t)$ under these conditions. His results together with those of Crank[20] yield the expression

$$\gamma_o(t) = \frac{\alpha}{g^2 t}\left[\mathrm{erfc}(g\sqrt{t})\,\exp(g^2 t) + 2g\sqrt{\frac{t}{\pi}} - 1\right] \tag{9a}$$

where t is the gas−liquid interaction time,

$$g = \frac{\alpha\bar{c}}{4HRTD_l^{1/2}} \tag{9b}$$

and D_l is the liquid-phase diffusion coefficient for the species. For details, see Robinson et al.[21]

It is possible to obtain a simple approximate expression for γ_o by decoupling solubility from mass accommodation. In the absence of surface reactions, γ_o is of the form

$$\frac{1}{\gamma_o(t)} = \frac{1}{\alpha} + \frac{1}{\Gamma_{sol}} \tag{10}$$

Here Γ_{sol} represents the effect on the uptake of Henry's law saturation and is approximately equal to

$$\frac{1}{\Gamma_{sol}} = \frac{\bar{c}}{8RTH}\sqrt{\frac{\pi t}{D_l}} \tag{11}$$

This approximate expression has been shown to be in good agreement with the Danckwerts formulation (eq 9). Specifically, a numerical comparison shows that eqs 10 and 11 yield values of α and H each within better than 13% of the values obtained using the more exact formulation of Danckwerts (see Robinson et al.[21]). Values for D_l used in the calculations were obtained from Houghton.[22] At 298 K, for ethanol, $D_l = 1.43 \times 10^{-5}$ cm^2 s^{-1} and for acetic acid, $D_l = 1.25 \times 10^{-5}$ cm^2 s^{-1}. The temperature dependence of D_l is given by Houghton.

Gas-Phase Diffusion. To our knowledge, gas-phase diffusive transport of a trace gas to a train of droplets has not been treated analytically. In fact, gas-phase diffusive transport does not lend itself to a straightforward analytical solution over the full range of Knudsen numbers even for a single stationary droplet. However, an empirical formulation of diffusive transport to a stationary droplet developed by Fuchs and Sutugin[23] has been shown to be in good agreement with measurements (see Widmann and Davis[24]). The expression for γ_{meas} in terms of the Fuchs−Sutugin formulation is most readily obtained from Widmann and Davis (their eq 48). That is

$$\gamma_{meas}(t) = \frac{1.333Kn}{1 + Kn\left\{\left(\frac{1.333Kn + 0.71}{1 + Kn}\right) + \frac{4(1 - \gamma_o(t))}{3\gamma_o(t)}\right\}} \tag{12}$$

Here the Knudsen number $Kn = 2\lambda/d_f$, the mean free path $\lambda = 3D_g/\bar{c}$, D_g is the gas-phase diffusion coefficient of the trace gas in the background gas, and γ_o, as defined earlier, is the uptake coefficient in the absence of gas-phase diffusion limitation. In the absence of surface reactions and solvation limitation imposed by Henry's law, $\gamma_o = \alpha$. For the case of a stationary droplet, d_f is simply the droplet diameter.

As was shown by Hanson et al.,[25] eq 12 is identically expressible in a form where the gas-phase diffusion term is decoupled from $\gamma_o(t)$ as

$$\frac{1}{\gamma_{meas}(t)} = \frac{3}{4}\left(\frac{1 + 0.377Kn}{Kn(1 + Kn)}\right) + \frac{1}{\gamma_o(t)} \tag{13}$$

The first term on the right-hand side (rhs) of eq 13 is $1/\Gamma_{diff}$.[26]

The central question is, can an expression derived for a stationary droplet properly account for gas phase diffusive transport to a train of moving droplets? The answer to this question could only be obtained experimentally, and the answer turned out to be yes.

As was stated earlier, experiments showed that diffusive transport to a train of closely spaced (typically 3−12 droplet diameters), moving droplets, produced by a vibrating orifice is well described by the Fuchs and Sutugin treatment (eq 13) with one key modification. The gas-phase transport is independent of droplet diameter but depends rather on the diameter of the droplet-forming orifice (d_o) such that in eq 13, $d_f = (2.0 \pm 0.1)$-d_o. This result is obtained from our most recently performed NH_3(g) uptake measurements on sulfuric acid droplets. These

diffusive transport studies, which will be described in an upcoming publication,[27] were performed over a wide range of Knudsen numbers ($Kn = 0.05$ to 4.5) with uptake coefficients ranging from 0.06 to 1. The droplet diameter was varied over a range of about a factor of 6. The results of our earlier studies,[13] performed over a narrower range of conditions, yielded $d_f = (1.9 \pm 0.1)d_o$, in good agreement with the newer measurements. We note further, that this relationship between d_f and d_o is not affected by droplet speed, which in the course of the experiments was varied by a factor 2.75 (from about 1600 to 4400 cm s^{-1}).

In our experiments, the walls of the flow tube are heated, and therefore the temperature of the gas is higher than the temperature of the droplets. The temperature used to calculate the gas-phase diffusion coefficient D_g was the average temperature between the droplet surface and the ambient gas. [13] It is also shown in ref 13 that the effect of this gradient on the droplet temperature is negligible. The values for the gas-phase diffusion coefficients used in eq 13 were calculated using CHEMKIN.[28] In units of atm cm^2 s^{-1}, at 294 K, the diffusion coefficients are $D_{HOAc-H_2O} = 0.094$; $D_{HOAc-He} = 0.423$; $D_{HOAc-Ar} = 0.090$; $D_{EtOH-H_2O} = 0.108$; $D_{EtOH-He} = 0.483$; $D_{EtOH-Ar} = 0.103$. These coefficients vary approximately as $T^{2.0}$. The exact dependence on temperature is given in the reference. The net diffusion coefficient D_g for a mixture of gases is calculated as discussed in Worsnop et al.[13]

Isotope Exchange at the Interface. Reactions specific to the gas−liquid interface, such as interfacial isotope exchange, open a new channel for the disappearance of the gas-phase species. In the case of isotope exchange at the interface it is useful to represent the process by the parameter p_{ex}, which is the probability that a molecule that strikes the liquid surface undergoes isotope exchange. We note that in the presence of isotope exchange at the interface two factors are responsible for the measured disappearance of the gas-phase species: (1) uptake into the bulk liquid of the gas-phase species that has not undergone isotope exchange (the probability for this process is $\alpha(1 - p_{ex})$) and (2) isotope exchange at the gas−liquid interface governed by probability p_{ex}. Therefore, in the absence of Henry's law solubility constraints, γ_o, the uptake coefficient with the effect of gas-phase diffusion removed, is

$$\gamma_o = \alpha(1 - p_{ex}) + p_{ex} \tag{14}$$

Here we have assumed that α's for the two species (isotope exchanged and unexchanged) are the same. With this assumption, as expected, the total uptake probability into the bulk liquid is unchanged. That is, the sum of the probabilities that the unexchanged species and the exchanged species enter the liquid is respectively $\alpha(1 - p_{ex}) + \alpha p_{ex} = \alpha$.

The unexchanged molecules that enter the bulk are of course subject to isotope exchanged within the liquid, but this does not add to the measured uptake of the species since the overall entry into the bulk is taken into account by the mass accommodation coefficient. However, isotope exchange within the bulk liquid is expected to be sufficiently rapid so that there is no evaporation out of the liquid of unexchanged molecules.[29]

The treatment of gas−liquid interactions via the electrical circuit analogy shown in Figure 1a has the advantage of allowing convenient inclusion of other interactions for which adequate exact treatments are not available. Isotope exchange at the interface is one such case. This process, as expressed in eq 14, can be included in the electrical circuit analogue, as shown in Figure 1b. In this figure Γ_{rxn} takes into account isotope exchange in the bulk liquid.[29]

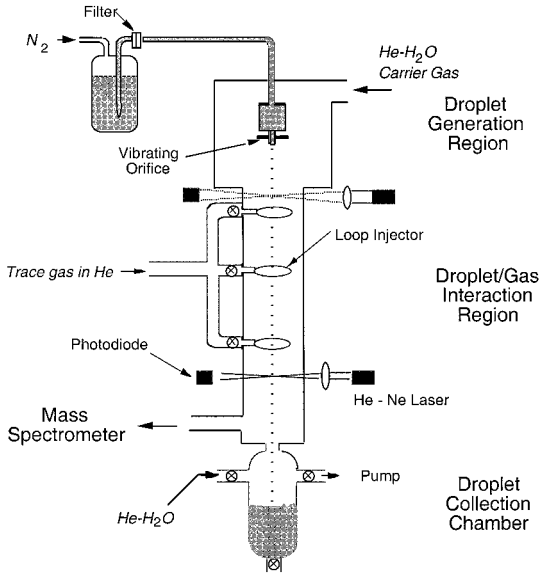

Figure 2. Droplet train apparatus.

The treatment of chemical reactions at the interface (here isotope exchange) in terms of a reaction probability is equivalent to a formalism introduced by Hanson[30] using a surface reaction coefficient Γ_s. The relationship between the two parameters is

$$\Gamma_s = p_{ex}/[(1 - \alpha)(1 - p_{ex})] \tag{15}$$

In the present experiments isotope exchange is studied as a function of pH. Therefore, isotope exchange may occur either directly with water molecules (the isotope exchange probability for this process is p_w), or via a catalytic interaction at the interface (with probability p_i) with ions (H^+ or OH^-). The total probability for isotope exchange can be shown to be

$$p_{ex} = p_w + (1 - p_w)p_i = p_w + p_i - p_w p_i \tag{16}$$

Experimental Method

The present uptake studies were conducted using a droplet train apparatus that was described previously[13] and is shown schematically in Figure 2. A fast-moving (1600−4400 cm/s), monodisperse, spatially collimated train of aqueous droplets was passed through a 30 cm long, longitudinal low pressure (6−20 Torr) flow tube that contains the trace gas species at a density between 5×10^{12} and 2×10^{14} cm^{-3}, entrained in a flowing mixture of helium and water vapor. The flowing carrier gases are introduced at the entrance of the reactor. The flowing trace gases are introduced through one of three loop injectors located along the flow tube. By selecting the gas inlet port and the droplet velocity, the gas−droplet interaction time can be varied between 2 and 15 ms.

The stream of droplets is produced in a separate chamber by a vibrating orifice. Two orifice sizes were used in these studies. In the alcohol experiments the orifices were 26 and 70 μm in diameter, generating droplets in the range 70−130 and 150−300 μm in diameter, respectively, depending on the frequency of orifice vibration. The acetic acid studies were conducted with orifices 28 and 64 μm in diameter.

Surface area of the droplets exposed to the trace gas in the flow tube is changed from A_1 to A_2 in a stepwise fashion by changing the orifice driving frequency. The density of the trace gas is monitored with a quadrupole mass spectrometer. The uptake coefficient (γ_{meas}) as defined by eq 3 is calculated from the measured change (Δn_g) in trace gas signal via eq 17.[13]

$$\gamma_{meas} = \frac{4F_g}{\bar{c}\Delta A} \ln \frac{n_g}{n_g'} \quad (17)$$

Here F_g is the carrier-gas volume rate of flow ($cm^3\ s^{-1}$) through the system, $\Delta A = A_1 - A_2$ is the change in the total droplet surface area in contact with the trace gas, and n_g and n_g' are the trace gas densities at the outlet of the flow tube after exposure to droplets of area A_2 and A_1, respectively ($n_g = n_g' + \Delta n_g$). Equation 17 is equivalent to the formulation used in heterogeneous wall loss flow reactor experiments. Here the surface-to-volume ratio is determined from the droplet train surface area, rather than from the surface area of the cylindrical flow tube.[13,31]

As stated earlier, in the presence of isotope exchange at the interface, two factors are responsible for the measured loss (disappearance) of the gas-phase species (Δn_g): uptake of the gas-phase species into the bulk liquid and isotope exchange at the gas−liquid interface. Since, in the presence of isotope exchange at the interface, the measured loss of the gas-phase species (Δn_g) includes the component that is not taken up by the liquid but rather is returned into the gas phase with D or H exchanged, γ in eq 17 should perhaps more accurately be called "loss coefficient". However, we will not make this change and retain our earlier nomenclature.

An important aspect of the experimental technique is the careful control of all the conditions within the apparatus. Water vapor pressure control in the droplet generation chamber and the flow tube is especially important. As was shown by Worsnop et al.,[13] the droplet surface equilibrates very quickly with the ambient vapor and therefore the surface temperature of the droplets is determined by partial pressure of water vapor. The water vapor is monitored using a calibrated electronic humidity probe. The present experiments are done with the water vapor pressure in the reaction zone between 1.44 and 17.5 Torr corresponding to temperatures between 258 and 293 K, respectively. At temperatures below 0 °C, the droplets are supercooled but not frozen.[13] Helium carrier gas is added to the water vapor at a partial pressure of about 3 Torr. Overall pressure balance in the flow tube is further checked by monitoring simultaneously the concentration of a reference gas, in this case krypton. Because krypton is effectively insoluble in water, any change in its concentration with droplet switching determines the "zero" of the system and is subtracted from observed changes in trace gas concentration. In earlier studies the system has been tested to ascertain that the droplet surface is not perturbed by the motion of the drop.[1]

Most of the measurements were performed with the 70 μm orifice. Studies with the 26 μm orifice were performed principally to confirm our treatment of gas phase diffusion and generally to test consistency of data. Uptake studies with the smaller orifice are intrinsically more difficult because of the greater drag on smaller droplets resulting in a more pronounced slow-down of droplets as they travel down the reaction zone. Therefore, in these experiments, the velocity of the droplets was measured by monitoring the transit time of droplets as the droplets interrupt laser beams in the droplet path at the top and bottom of the reaction zone. This time interval is obtained by timing the droplet train as the size of the droplets is changed in a stepwise manner.

The decrease in speed of droplets generated with the 70 μm orifice is 5.5 (cm/s)/cm, resulting in a total decrease in speed of only 5% along the 21 cm reaction zone. On the other hand, for the smaller droplets generated with the 26 μm orifice the decrease in speed along the 21 cm reaction zone is 23% and has to be taken into account in calculating the uptake.

Since water vapor is continually present in the reaction zone, effects on the isotope exchange process of trace gas collisions with water molecules and with the walls of the flow tube had to be carefully assessed. We have shown that for ethanol, isotope exchange due to collisions between gas phase species is negligible. However, collisions with the wall can indeed produce isotope exchange. Wall loss was measured by monitoring the decrease of the deuterated ethanol signal (mass 52), in the absence of droplets, as a function of distance from the detector. During these measurements all other conditions in the flow tube were identical to those set for droplet uptake measurements. On clean walls isotope exchange for ethanol is modest. Expressing wall loss in the form $\exp(-ax)$, where x is the distance along the flow tube, the parameter "a" for a clean wall is typically 0.009 cm^{-1}. The equivalent loss parameter for the droplets themselves can be calculated from γ_{meas} via eq 17 and it is in the range 0.05 cm^{-1}. The loss parameter increases significantly for a wall contaminated by splattered acidified or basic droplets. We measured the uptake under a variety of wall conditions. The studies included conditions where the walls were purposely contaminated and where they were coated with the compound $C_{14}H_{19}F_{13}O_3Si$ or halocarbon. Studies were conducted with walls heated from room temperature to 50 °C. Depending on conditions, the parameter "a" in these studies varied from a = 0.009 to 0.05 cm^{-1}.

As stated earlier, in our experiment the change in the trace gas density is monitored as the area of liquid droplets in the reaction zone is altered in a stepwise manner. Therefore, in principle, the depletion signal due to gas−droplet interaction should be independent of wall loss. A detailed set of uptake studies showed that this is indeed the case for alcohol over the range of wall conditions studied. Still optimum signal-to-noise is obtained at the lowest wall losses and our reported measurements were conducted under low wall loss conditions.

Isotope exchange is significantly more facile for deuterated acetic acid than for alcohol. Consequently, wall losses are also higher. In fact, isotope exchange on the walls for this species was so large (a = 0.05 cm^{-1}) that quantitative measurements could be obtained only at low water vapor pressures corresponding to low droplet temperatures. Further, instead of helium, argon had to be used as the carrier gas in order to decrease diffusive transport to the walls. These factors, of course, limited the range of measurements. Still, to facilitate comparison with the alcohol measurements, experiments were conducted in overlapping region of Knudsen numbers.

The deuterated species were obtained from Cambridge Isotope Laboratories, Inc. and the nondeuterated from Aldrich Chemical Co. Inc. The species were diluted in helium and were used without further purification. The density of the gas-phase species in the flow tube was varied from 5×10^{12} to 2×10^{14} cm^{-3}. The density of Kr was in the same range. The low and high pH droplets were prepared with sulfuric acid and NaOH, respectively. In the study with deuterated water droplets, the low pH was set with deuterated sulfuric acid.

The following experiments were performed:

1. The uptake (disappearance) of normal and fully deuterated gas-phase acetic acid in contact with water (H_2O) droplets was measured at pH 7 and 258 K with 64 and 28 μm diameter droplet generating orifices.

2. The uptake (disappearance) of normal gas-phase ethanol (mass 46) and fully deuterated ethanol (mass 52) in contact with water (H_2O) droplets was measured as a function of pH in the range 0−14 and gas−liquid interaction time in the range 2−15 ms with both the 70 μm and the 26 μm diameter droplet-

generating orifices. Measurements with the 70 μm orifice were performed at droplet temperatures 291, 283, 273, and 263 K. The data obtained at 263 K were limited to two pH values, 7 and 0. Uptake studies with the 26 μm orifice as a function of pH were performed at one temperature only, at 273 K.

3. To confirm mass balance, in a limited set of deuterated ethanol studies, both the disappearance of mass 52 deuterated ethanol and the appearance of the isotope-exchanged mass 51 ethanol were monitored. (As is well-known and as was confirmed in our experiments, only the deuterium associated with the oxygen atom undergoes exchange.) In these studies the initial density of the deuterated ethanol (mass 52) at the gas inlet point ($x = 0$) was established by measuring the intensity of the 52 and 51 masses in the absence of droplets. With the droplets off, mass 51 ethanol is produced by isotope exchange on the walls of the flow tube along the full length (l) from the inlet to the mass spectrometer. The mass 52 signal at the $x = 0$ inlet position is obtained simply by summing the measured mass 51 and 52 signals. An independent check on the validity of this approach is obtained by computing the expected mass 51 signal using the previously measured wall loss coefficient "a" (that is, [mass 51] = [Mass 52($x = 0$)] $\times$ [1 $-$ exp($-al$)]). Then, the intensity of the mass 51 and 52 signals are measured with the droplets on. In this case, the additional mass 51 ethanol is due to the fraction of the isotope-exchanged species on or in the droplets that returns and remains in the gas phase. By mass balance, the difference between the initial mass 52 signal and the sum of the final mass 52 and 51 signals is the fraction that entered and remained in the droplets. This fraction can be computed independently if the values of α and H are known. In what follows we assumed that values of α and H for normal and deuterated ethanol are the same. The fraction that entered and remained in the droplets is then calculated using the uptake coefficients γ_{meas} measured in the experiments with normal ethanol. The mass balance studies were done at 0 °C with the 70 μm droplet-generating orifice at pH 2 and pH 7.

4. The uptake of normal gas-phase ethanol in contact with deuterated water (D_2O) droplets was measured at pH 1 and 7 as a function of gas$-$liquid interaction time in the range 2$-$15 ms. Measurements were performed at 273 K with the 70 μm droplet generating orifice. The range of these studies was limited because of the expense involved in using deuterated water.

5. Exploratory uptake studies were conducted with trifluoroethanol, 2-chloroethanol, and D_2S to determine the nature of the isotope exchange process for a wider range of species.

Results and Analysis

Acetic Acid. As an example of uptake measurements with acetic acid, we show in Figure 3 a plot of $\ln(n_g/n_g')$ for deuterated acetic acid as a function of $\bar{c}\Delta A/4F_g$ at 258 K (supercooled) and pH = 7. Here $\bar{c}\Delta A/4F_g$ was varied by changing the droplet surface area (ΔA). Each point is the average of at least 10 droplet area change cycles. The error bars in this, and all other figures, represent one standard deviation (68% confidence level) in the experimentally measured $\Delta n/n$ value. As is evident in eq 17, the slope of the plot in Figure 3 yields the value of γ_{meas}. In these studies the uptake signal $\Delta n_g/n_g$ varied typically from 5% to 30%.

Uptake measurements with acetic acid were conducted as a function of gas$-$droplet contact time. Henry's law constant for acetic acid is high ($H = 8000$ M atm^{-1} at 298 K), and therefore, as expected, in accord with eqs 9 or 11, in the range of gas$-$liquid interaction times of these experiments (2$-$15 ms), γ_{meas} did not exhibit time dependence.

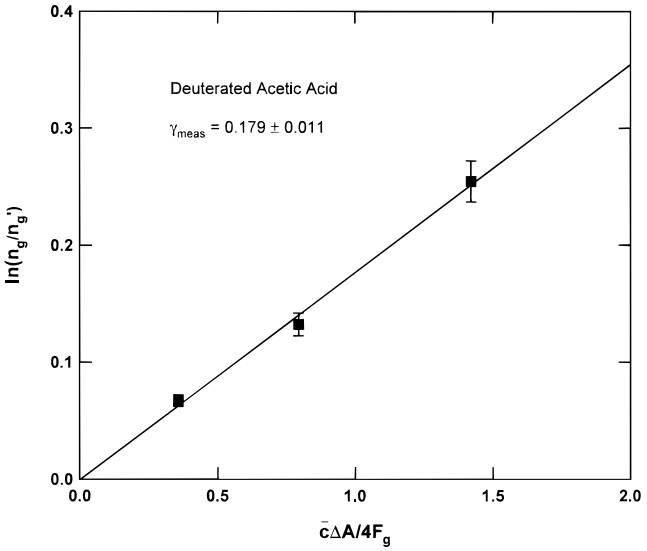

Figure 3. Plot of $\ln(n_g/n_g')$ for deuterated acetic acid as a function of $\bar{c}\Delta A/4F_g$ at droplet temperature $T_d = 258$ K and pH = 7. Slope of the line is γ_{meas}. Terms are defined in the text.

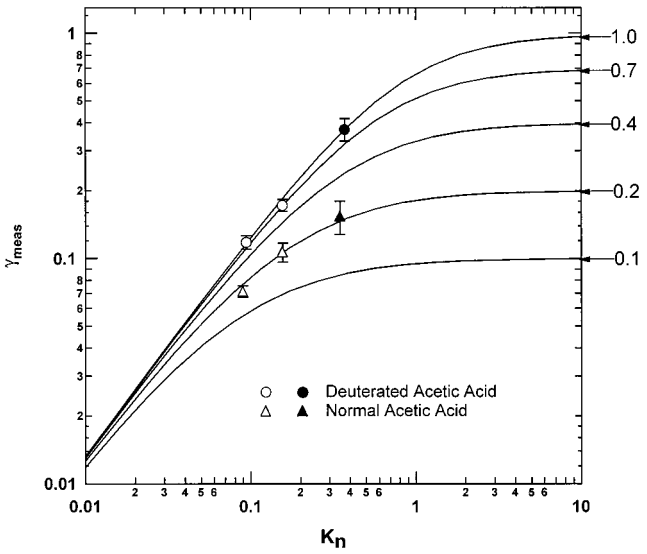

Figure 4. γ_{meas} vs Kn for acetic acid at 258 K. The solid lines are plots of the Fuchs and Sutugin equation (eq 13) with γ_o as the parameter. Circles and triangles are uptake coefficients for deuterated and normal acetic acid, respectively. Open circles and triangles were obtained with the 64 μm diameter orifice. The filled circle and triangle were obtained with the 28 μm diameter orifice.

In Figure 4 we show γ_{meas} for normal and deuterated acetic acid displayed as a function of Kn. The solid lines are plots of the Fuchs and Sutugin equation (eq 13) with γ_o as the parameter. The circles and triangles are the measured uptake coefficients for deuterated and normal acetic acid, respectively. The γ_{meas} values represented by the open circles and triangles were obtained with the 64 μm droplet-forming orifice. The filled circle and triangle were obtained with the 28 μm orifice. The 64 μm results at the higher Kn were obtained under normal operating pressure conditions. As an additional test of our treatment of gas-phase diffusion, a second set of 64 μm results was obtained at lower Kn by purposely increasing the argon carrier gas pressure. As is evident, the uptake coefficients for normal acetic acid consistently fall on the line $\gamma_o = \alpha = 0.19(\pm 0.03)$ whereas the uptake coefficients for deuterated species fall on the line $\gamma_o = 0.96(\pm 0.21)$. The fact that we can observe $\gamma_o = 1$ in this case shows that lower uptake values measured for other species,

TABLE 1: Mass Balance for Deuterated Ethanol Uptake at pH = 2 and 7 and T_d = 0 °C

	pH = 2			pH = 7		
	low inlet	mid inlet	high inlet	low inlet	mid inlet	high inlet
normalized initial mass 52 at the gas inlet $x = 0$	1	1	1	1	1	1
1. normalized final mass 52 signal	0.54	0.38	0.25	0.58	0.45	0.33
2. normalized final mass 51 signal	0.36	0.37	0.4	0.33	0.33	0.34
3. fraction of mass 52 and 51 into droplets[a]	0.12	0.25	0.36	0.12	0.25	0.36
1 + 2 + 3	1.02	1.00	1.01	1.03	1.03	1.03

[a] Calculated using γ_{meas} for normal ethanol.

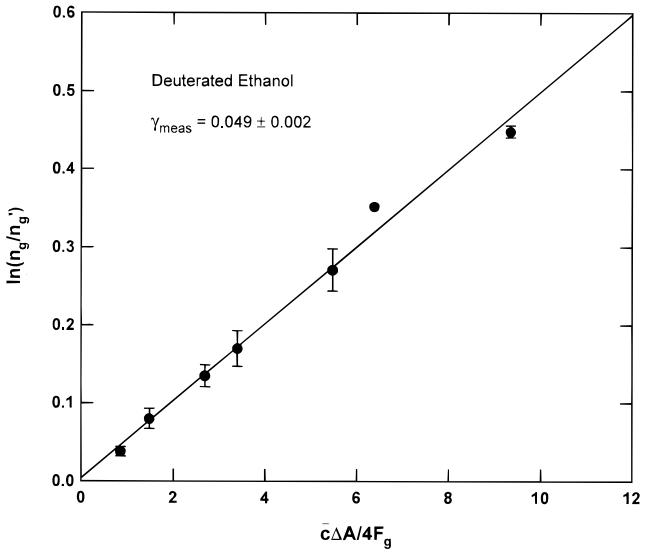

Figure 5. Plot of $\ln(n_g/n_g')$ for deuterated alcohol as a function of $\bar{c}\Delta A/4F_g$ at droplet temperature $T_d = 283$ K and pH = 7.

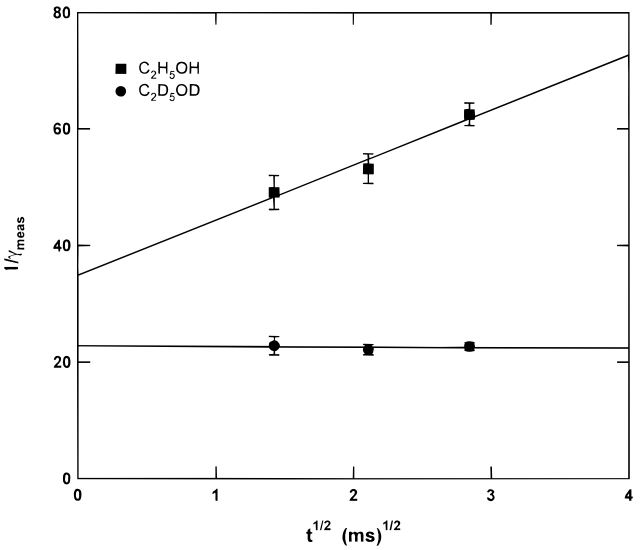

Figure 6. $1/\gamma_{meas}$ as a function of $t^{1/2}$ for normal and fully deuterated ethanol in contact with water (H_2O) droplets. (t is gas−liquid interaction time.) $T_d = 291$ K and pH = 7.

under similar conditions, are not due to an experimental limitation in our ability to measure uptake rates.

We note that at low values of *Kn*, an uncertainty in the value of *Kn* can have a large effect on the magnitude of γ_o extracted from γ_{meas}, as is evident from the slope of the plot in Figure 4. However, the uncertainty decreases as *Kn* increases so that at $Kn = 0.37$ (the largest *Kn* values in the figure) a 10% change in *Kn* results in a change in γ_o of 4% at $\gamma_o = 0.2$ and 19% at $\gamma_o = 1$.

Ethanol. Ethanol uptake measurements were performed as a function of gas−droplet contact time, droplet temperature, and droplet pH. As an example of the measurements, we show in Figure 5 a plot of $\ln(n_g/n_g')$ for deuterated alcohol as a function of $\bar{c}\Delta A/4F_g$ at 283 K and pH = 7. As before, the slope of the plot yields the value of γ_{meas}.

Uptake as a Function of Gas−Liquid Interaction Time. In contrast with acetic acid, the uptake of normal alcohol on H_2O droplets does exhibit a time dependence on the millisecond experimental time scale of the apparatus. This is evident in Figure 6, where uptake data are shown in the form $1/\gamma_{meas}$ vs $t^{1/2}$ for normal and fully deuterated ethanol in contact with water (H_2O) droplets. (t is the gas−liquid interaction time.) The measurements shown were obtained at 291 K and pH = 7. The time dependence in the uptake of normal alcohol is clearly evident. In accord with eqs 10 and 11, the slope of the line is $(\bar{c}/8HRT)(\pi/D_l)^{1/2}$, yielding $H = 325$ M atm^{-1}. This is in excellent agreement with the literature value of $H = 334$ M atm^{-1}.[32] Because of increasing solubility, the time dependence of the alcohol uptake decreases at lower droplet temperatures. Note that the $t^{1/2} = 0$ intercept of Figure 6 yields the value of the uptake coefficient at $t = 0$ where solubility does not limit the uptake. It is through such extrapolation that we obtain uptake coefficients free of Henry's law solubility constraints.

In contrast with normal ethanol, the uptake coefficient for deuterated ethanol is not a function of gas−liquid interaction time. This is in accord with expectations, since a deuterated alcohol that enters the liquid rapidly exchanges with hydrogen within the liquid so that there is no evaporation out of the liquid of the fully deuterated species. The situation is equivalent to having a fast reactive sink within the bulk liquid.

Mass Balance. Results of the mass balance studies are summarized in Table 1. As discussed above, the initial mass 52 and final mass 52 (numbered 1 in the table) and 51 signals (numbered 2) are obtained from measurements and are tabulated in a normalized form. As discussed earlier, the fraction of mass 52 and 51 ethanol entering and remaining in the droplets is calculated using the uptake coefficients γ_{meas} measured in the experiments with normal ethanol (numbered 3). As is evident, the sum of entries 1 + 2 + 3 establishes mass balance to better than 4%. This also confirms the assumption that the mass accommodation coefficients for normal and deuterated ethanol are the same.

Ethanol Uptake. The uptake coefficient γ_{meas} at $T = 273$ K as a function of pH for normal and fully deuterated ethanol in contact with water (H_2O) droplets is shown in Figure 7. The plotted γ_{meas} values include the effect of gas-phase diffusive transport. However, in this figure (as well in Figures 8−10), the plotted uptake coefficients for normal ethanol are values extrapolated to $t = 0$ so that the effect on the uptake of Henry's law solubility constraint is removed (see eqs 4 and 11). Uptake data for deuterated ethanol obtained with both 26 and 70 μm droplet-generating orifices are shown in Figure 7. As expected, the 26 μm orifice yields larger values of γ_{meas} because diffusive transport to smaller droplets is faster (larger values of Γ_{diff}). In

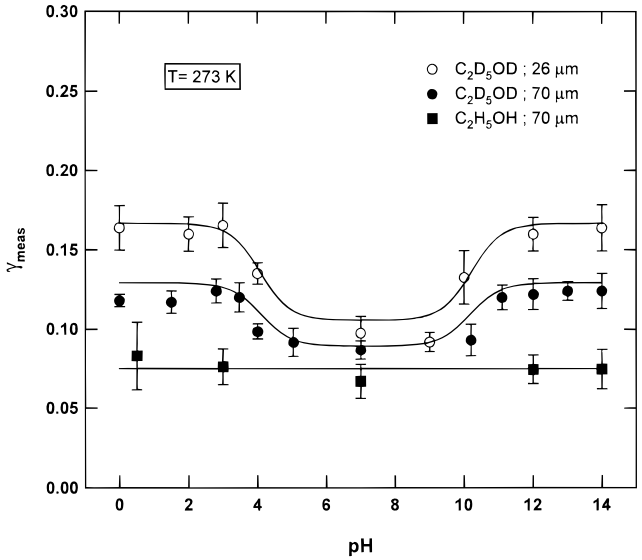

Figure 7. Uptake coefficient γ_{meas} as a function of pH for normal (■) and fully deuterated ethanol in contact with water (H_2O) droplets. Uptake data for deuterated ethanol were obtained with both 26 μm (○) and 70 μm (●) droplet-generating orifices. $T_d = 273$ K. The plotted uptake coefficients for normal ethanol are values extrapolated to $t = 0$. (See text.)

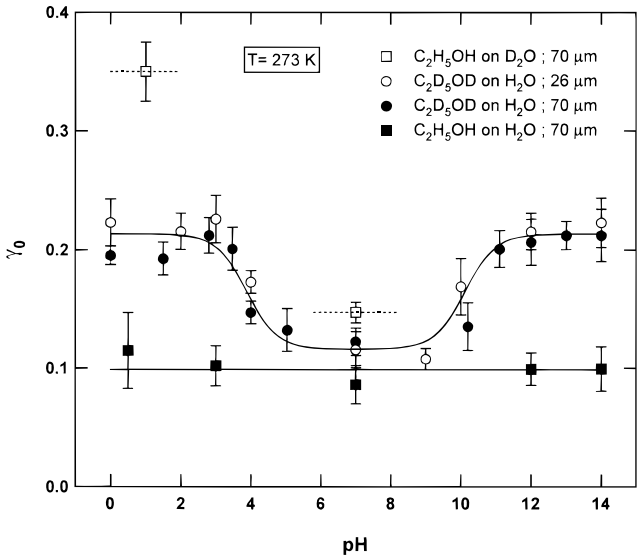

Figure 8. Gas-phase diffusion-corrected uptake coefficients γ_o as a function of droplet pH for normal (■) and fully deuterated ethanol in contact with aqueous (H_2O) droplets. Uptake data for deuterated ethanol were obtained with both 26 μm (○) and 70 μm (●) droplet-generating orifices. Uptake data for normal ethanol (□) in contact with deuterated water (D_2O) droplets were obtained at pH = 1 and 7 with 70 μm droplet-generating orifices. $T_d = 273$ K. The plotted uptake coefficients for normal ethanol are values extrapolated to $t = 0$. (See text.)

these and the other determinations of uptake coefficients, each γ is the result of at least three independent uptake runs.

The uptake coefficient γ_o, free of gas-phase diffusion transport limitation, is obtained via eq 13. This quantity for deuterated ethanol at 273 K is shown as a function of pH in Figure 8. As is evident in the figure, with gas-phase diffusion taken into account, the uptake data obtained with the 26 and 70 μm droplet-generating orifices are in good agreement with each other. The solid line is based on a model discussed in the next section. The gas-phase diffusion-corrected uptake coefficients γ_o for deuterated ethanol as a function of pH at 283 K and 291 K are shown in Figures 9 and 10.

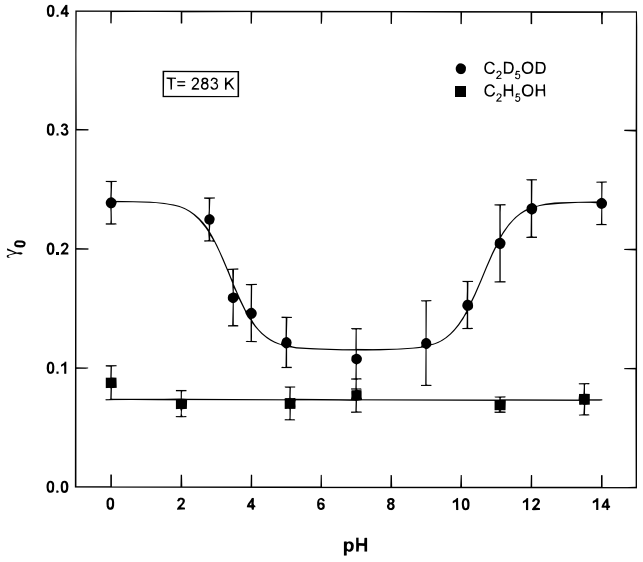

Figure 9. Gas-phase diffusion-corrected uptake coefficients γ_o as a function of pH for normal (■) and fully deuterated (●) ethanol in contact with water (H_2O) droplets. $T_d = 283$ K. The plotted uptake coefficients for normal ethanol are values extrapolated to $t = 0$. (See text.)

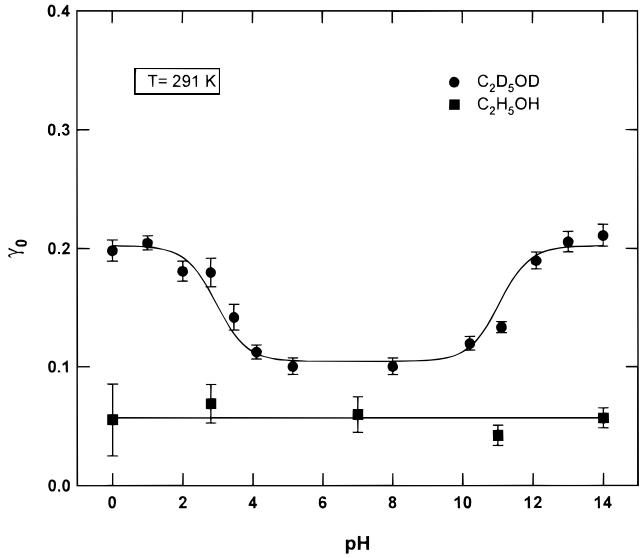

Figure 10. Gas-phase diffusion-corrected uptake coefficients γ_o as a function of pH for normal (■) and fully deuterated (●) ethanol in contact with water (H_2O) droplets. $T_d = 291$ K. The plotted uptake coefficients for normal ethanol are values extrapolated to $t = 0$. (See text.)

In Figure 8 we also shows the two γ_o values at pH 1 and 7 obtained from the measured uptake of normal ethanol on D_2O. As is evident, the γ_o value at the plateau is here about a factor of 1.6 higher than the plateau value for deuterated ethanol.

In Table 2 we list the salient parameters obtained from the uptake measurements. These are the mass accommodation coefficient α, the gas-phase diffusion-corrected uptake coefficient at the plateau designated as γ_{o-p}, the diffusion-corrected uptake coefficient at pH 7, and the isotope exchange probabilities at the uptake plateau (p_{ex-p}) and at pH 7 (p_w), calculated via eq 14. The table includes values obtained from the limited set of measurements at 263 K, as well as the results from the uptake measurements of normal ethanol on deuterated water obtained at 273 K. The results for deuterated alcohol on normal water and normal ethanol on deuterated water are designated as (D→H) and (H→D), respectively.

TABLE 2: Parameters for Ethanol Uptake Obtained from Measurements[a]

		263 K	273 K	283 K	291 K
α		0.128 ± 0.023	0.100 ± 0.010	0.075 ± 0.003	0.057 ± 0.005
γ_{o-p}	(D→H)	0.246 ± 0.020	0.208 ± 0.006	0.240 ± 0.004	0.202 ± 0.005
	(H→D)		0.350 ± 0.025		
γ_o(pH = 7)	(D→H)	0.157 ± 0.020	0.122 ± 0.006	0.116 ± 0.020	0.105 ± 0.004
	(H→D)		0.147 ± 0.009		
p_{ex-p}	(D→H)	0.135 ± 0.046	0.120 ± 0.016	0.178 ± 0.007	0.154 ± 0.010
	(H→D)		0.280 ± 0.036		
p_w	(D→H)	0.033 ± 0.010	0.024 ± 0.004	0.044 ± 0.009	0.051 ± 0.006
	(H→D)		0.052 ± 0.008		

[a] Error limits are one standard deviation.

Exploratory uptake studies were conducted with deuterated trifluoroethanol, 2-chloroethanol, and D_2S on water. The uptake results for deuterated trifluoroethanol and 2-chloroethanol were similar to those obtained with ethanol. Isotope exchange was not observed in the studies with D_2S.

Discussion

Acetic Acid Uptake. For normal acetic acid the uptake coefficient γ_o obtained from the plot in Figure 4 is simply the mass accommodation coefficient α. This newly measured value of $\alpha = 0.19 \pm 0.03$ at 258 K is somewhat higher but is within 1σ of $\alpha = 0.15 \pm 0.03$ measured in our earlier studies.[16] The difference is most likely due to the more accurate determination of the water vapor partial pressure, which affects the gas flow rate and droplet temperature.

The uptake coefficient γ_o for deuterated acetic acid is, within experimental accuracy, unity, indicating that the isotope exchange probability (p_w) with water molecules at the interface is likewise near this value. This is not surprising. Two factors may contribute to the facile D−H exchange for this species. First, the acidic nature of the species promotes the relatively facile departure of deuterium. Second, since the two oxygens of acetic acid are resonant, the deuterium from the hydroxyl site can rapidly depart toward a neighboring H_2O while the H atom from that water molecule forms a bond with the other oxygen. We note that facile proton exchange was also observed for DCOOD and D_2O in molecular beam scattering experiments on concentrated (98.8 wt %) sulfuric acid films.[7,6]

Ethanol Uptake. The uptake coefficients γ_o for the normal ethanol shown in Figures 8−10 are simply the mass accommodation coefficients α and, as expected, they are independent of pH. These newly measured values of α are again higher than were measured in our earlier studies,[16] but are within 2σ of the earlier values. Here again the current measurements are considered more accurate.

In connection with the deuterated ethanol uptake studies, we first note from Figure 8 that the uptake studies with the two orifices 26 and 70 μm in diameter, yield γ_o values in good agreement with each other. Since diffusive transport is enhanced for smaller droplets, the fact that identical treatment of gas-phase diffusion for droplets of diameters differing by a factor of 2.7 yields the same uptake coefficients γ_o, is a further validation of our understanding of diffusive transport.

The pattern in the uptake data for the deuterated ethanol undergoing isotope exchange is clearly evident; its uptake coefficient is always larger than that for normal ethanol. It could be argued that in the flat region around pH 7, this larger uptake is due to a larger α for the deuterated species. However, we believe that this is not the case, principally for two reasons. First, the temperature dependence for the deuterated ethanol γ_o at pH 7 is significantly smaller than measured for α of normal alcohol. As is shown in Table 2, from 291 to 263 K α increases by a factor of 2.2, whereas γ_o for deuterated ethanol increases only by a factor of 1.5. Second, at 291 K the magnitude of γ_o for deuterated ethanol is almost twice as large as the α of normal alcohol. Such a large difference in the mass accommodation process for the two species is not likely. As stated earlier, we assume that α for the two species is the same, and the fact that γ_o is always greater than α is due to the additional channel for species disappearance as result of isotope exchange at the interface.

As is evident in the figures, γ_o increases both toward low and high pH, reaching a plateau of the same value at both ends. While some isotope exchange does occur with water molecules, exchange is significantly enhanced with solutions at high and low pH. This additional uptake (loss) of the labeled ethanol can be attributed to catalytic interactions with OH^- and H^+. As will be shown, in the region of increasing γ_o, the enhanced uptake (loss) due to acid- and base-catalyzed isotope exchange shows a linear dependence on H^+ and OH^- concentrations. It is important to note that such linear dependence points to an uptake governed by surface reactions as opposed to bulk reactivity, which is proportional to the square root of the reactant concentration.[29]

The observed plateaus in the uptake as a function of pH hold a key to understanding the nature of isotope exchange at the interface. We certainly did expect a plateau in the uptake at low and high pH since surface reactions reach a limit in the region where the density of reactive surface sites is sufficiently high so that every molecule that strikes the surface might be subject to reaction. However, we expected under these conditions the probability of reactive interaction to be unity, and correspondingly, we expected the plateau to occur near a value of $\gamma_o = 1$. Clearly, in our studies the magnitude of γ_o at the plateau is less than 1. For the deuterated ethanol interacting with water it is about 0.22 and for normal ethanol interacting with deuterated water it is about 0.35. In this respect surface isotope exchange is very different for ethanol than for the acetic acid where the isotope exchange probability even on a pure water surface is unity.

For both acetic acid and ethanol we have reproduced our earlier uptake measurements and have shown that the isotope exchange process at the interface further increases the species uptake (loss). These results confirm our previous studies, which indicate that mass accommodation coefficients for trace gases on liquid water are in general less than unity, that is, $k_{sol}/k_{des} < 1$ (see eq 8).

The results for acetic acid clearly distinguish interfacial and gas diffusion resistance to uptake. Here, at 258 K, α is 0.2 for uptake into solution, while for labeled acetic acid uptake is gas diffusion limited, with maximum $\gamma_{meas} = 0.4$, implying a value of $\gamma_o = 1$, due to fast D−H isotope exchange reaction for the acid on water (see Figure 4). The results for EtOD uptake likewise distinguish interfacial and gas diffusion resistance

except that γ_o does not approach unity. The observation of a $\gamma_o < 1$ plateau in the limit of high H^+ or OH^- concentrations implies that there is a barrier between the vapor and solution even for surface reaction. A kinetic model of the gas−liquid interface will have to take into account this additional complexity revealed by the present experiments.

A plateau of less than 1 in the uptake coefficient is not unique to the isotope exchange process. In an earlier experiment we studied the uptake of gas-phase Cl_2 and Br_2 by aqueous solutions containing halogen ions I^- and Br^-.[11] Although the Hu et al. study presented a somewhat different formulation of surface reactivity, the observation of $\gamma_o < 1$ in the limit of high halide concentration is exactly equivalent to the plateau observed here. In that case, the transition from bulk to surface reactivity was clearly resolved as a function of low to high reactant ion concentration (10^{-3} to 1 M). At 273 K the plateau value of γ_o was respectively 0.2 and 0.017 for the Br_2/I^- and Cl_2/I^- uptake processes.

The new aspect of the present experiments is the distinguishable observation of both α and surface reactivity for EtOH and isotopically labeled EtOD. The detailed and most complete picture of surface reactivity provided by the experiments of Hanson and Ravishankara[9] for the $ClONO_2 + HCl$ reaction in sulfuric acid solution clearly delineated bulk reaction with H_2O and HCl from surface reaction with HCl. However, that work was performed at 203 K where $\alpha = 1$, with no possibility of observing the interfacial barrier investigated in this work.

The following model for the H^+ or OH^- catalyzed isotope exchange process provides a possible explanation for the observed results.

Kinetic Model of the Gas-Liquid Interface

Loss of unlabeled ethanol is due to one process only, solvation. On the other hand, labeled ethanol molecules can undergo two additional processes: (1) Isotope exchange with water molecules on the surface and (2) Isotope exchange via acid or base catalysis. The fact that the uptake plateau (γ_{o-p}) is smaller than unity leads us to modify the reaction scheme in eq 5 by assuming that the surface adsorbed ethanol molecules designated as n_s, are distributed between two distinct forms; a weakly adsorbed state (n_w), and a partially solvated state (n_p). Such a picture of the interface is directly analogous to discussion of n_s and n_s* surface states to represent α in the mass accommodation process.[2]

Molecular dynamics calculations[33] show that there is a substantial barrier for ions to approach the surface of water beginning about 0.8 nm (or two to three molecular diameters) from the surface. We postulate that this barrier prevents the ion-catalyzed isotope exchange from occurring with the weakly adsorbed molecules, n_w. We suggest that an ethanol molecule must enter a partially solvated state n_p before it can interact with the near-surface ions in the interior of the liquid. If this is the case, then a finite rate of entering the partially solvated state is responsible for the observed plateaus in uptake at high and low pH. Of course, this assumption of a specific partially solvated state is a simplification; in reality, there must be a continuum of states that exists as a molecule enters the liquid and becomes fully solvated.

Let k_f be the rate of transfer from the weakly adsorbed state to the partially solvated state and let k_b be the reverse rate constant. Molecules in the weakly adsorbed state can undergo direct isotope exchange with rate constant k_E. The partially solvated molecules can enter the fully solvated state, with rate constant k_2, or undergo isotope exchange, with rate constant k_R. (A fraction of the molecules that has undergone isotope exchange may then also enter the fully solvated state.) In general, we expect that k_R should include a term for uncatalyzed exchange (k_o) and terms for acid- and base-catalyzed exchange (k_c). Although the acid- and base-catalyzed reactions may proceed with slightly different rate constants,[34,35] the present data are insufficient to make this distinction. We therefore express k_R via

$$k_R = k_o + k_C([H^+] + [OH^-]) \tag{18}$$

This formulation of uptake, controlled by surface reaction, assumes that the parameters governing uptake are linear in the surface reaction rate k_E or k_R and thus are linear in the reactant concentration as in eqs 18 and 19. As is discussed in the previous surface reactivity studies,[11] it is the linear dependence of the uptake parameters on reactant concentration that distinguishes surface reactivity from bulk reactivity. Gas uptake governed by liquid-phase diffusion controlled bulk reactivity exhibits a square root dependence on reactant concentration.[9−12]

We can summarize this reaction scheme as follows:

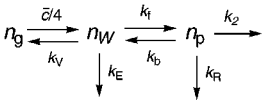

(19)

The total species surface density n_s in eq 5 is

$$n_s = n_w + n_p \tag{20}$$

As noted above, the reaction scheme in eq 19, involving two surface states, is analogous to the one developed to account for mass accommodation,[2] with the partially solvated species n_p to be identified with n_s* in that work. Labels and subscripts have been changed to clarify the more general treatment of the process presented here. The major difference between eq 19 and the mass accommodation formulation is the inclusion of the k_E and k_R terms here to account for surface reactions that were not considered previously.[36]

Using the reaction scheme in eq 19 and applying the steady state approximation to the partially solvated and weakly adsorbed states, we obtain the following expression for the uptake coefficient:

$$\gamma_o = \frac{(k_f + k_E)(k_2 + k_R) + k_E k_b}{(k_f + k_E + k_V)(k_2 + k_R) + (k_E + k_V)k_b} \tag{21}$$

It is evident that eq 21 predicts a plateau in uptake at very high and very low pH as $k_R \rightarrow \infty$. The value of this limiting uptake coefficient, γ_{o-p}, is

$$\gamma_{o-p} = \frac{k_f + k_E}{k_f + k_E + k_V} \tag{22}$$

with k_R and k_E set to zero, eq 21 yields α as

$$\alpha = k_f k_2/[(k_f + k_V)k_2 + k_V k_b] \tag{23}$$

As before, in what follows we will assume that the mass accommodation coefficient for labeled and unlabeled ethanol is the same.

The rate of desorption of weakly adsorbed molecules k_V, is related to overall desorption rate k_{des} in eq 5 by

$$k_V = k_{des}(1 + K) \tag{24}$$

TABLE 3: Kinetic Parameters Obtained from the Model Fit[a]

		263 K	273 K	283 K	291 K
k_2/k_b	(D→H)	1.048 ± 0.010	0.90 ± 0.12	0.440 ± 0.020	0.441 ± 0.036
	(H→D)		0.303 ± 0.098		
k_f/k_V	(D→H)	0.287 ± 0.095	0.235 ± 0.031	0.265 ± 0.014	0.198 ± 0.022
	(H→D)		0.477 ± 0.075		
k_C/k_b (M^{-1})	(D→H)		9200 ± 4800	3000 ± 600	1200 ± 400
k_E/k_V	(D→H)	0.039 ± 0.059	0.027 ± 0.032	0.051 ± 0.016	0.055 ± 0.023
	(H→D)		0.061 ± 0.024		

[a] Error limits are one standard deviation.

where K is the equilibrium constant for the weakly adsorbed and partially solvated states given by

$$K \equiv k_f/k_b \tag{25}$$

By rearranging eq 8 we obtain

$$k_{sol} = k_{des}\alpha/(1-\alpha) \tag{26}$$

From which, via eq 23, we obtain the overall solvation rate k_{sol} as

$$k_{sol} = \frac{k_f k_2}{(1+K)(k_b + k_2)} \tag{27}$$

The phenomenological surface interaction parameters p_{ex} and Γ_s defined in eqs 14 and 15, can be expressed in terms of the rate coefficients presented above, via eqs 21 and 23.

Equation 21, together with eq 18, depends on seven unknown rate constants. All terms in eq 21 are products of one rate constant that applies to the weakly adsorbed state and one for the partially solvated state. We can divide the former set of rate constants by k_V and the latter set by k_b to reduce the number of parameters by 2. Further, while it is likely that in general uncatalyzed isotope exchange occurs both in the weakly adsorbed and partially solvated states, in the calculations that follow, we will assume that this process occurs entirely in the weakly adsorbed state, i.e., $k_o = 0$. Calculations show that the other parameters are not affected significantly by this assumption. At this point without further assumptions, we can obtain ratios of rate constants, namely, k_2/k_b, k_f/k_v, k_c/k_b, and k_E/k_b, by a nonlinear fit to the experimental data shown as solid lines in Figures 7−10. The rate constant ratios for the limited set of deuterated ethanol measurements at 263 K and the normal ethanol on D_2O measurements were calculated from the values of γ_{o-p}, γ_o(pH = 7), and α (eqs 22 and 23). The results are shown in Table 3.

As is evident, the quality of the solid line fits in Figures 8−10 provided by the kinetic model presented is very good. Of particular importance is the fit to the data in the pH regions where the uptake is increasing with the reactant (OH^- or H^+) concentration. Only a linear dependence on the acid and base concentration consistent with the surface reaction model can provide an adequate fit to the data. The quality of the fits also provides further confirmation for the assumption that the mass accommodation coefficient for both the labeled and unlabeled ethanol molecules is the same.

We note again the uptake behavior of acetic acid in contrast to that of ethanol. The observation that α for acetic acid is less than 1, while the uptake coefficient γ_o of the labeled species is about unity, even at pH 7, implies that isotope exchange for acetic acid is facile, occurring directly with water in the weakly adsorbed state. Since $\gamma_o = 1$, eq 22 implies that k_E (the isotope exchange rate for the weakly solvated state) is much larger than ($k_f + k_v$). As stated in the Discussion, the facile isotope exchange for acetic acid is most likely due to the acidic nature of the species and the resonant structure of the two oxygens of acetic acid.

The only clearly interpretable result for ethanol is provided by the ratio k_2/k_b, which is about unity at 263 K and decreases as the temperature increases. Thus, at higher temperatures it is more likely that the partially solvated molecules return to the weakly adsorbed state rather than becoming fully solvated. This implies that as the temperature increases, the partially solvated state more closely resembles the adsorbed state than the bulk state.

As was pointed out, γ_{o-p} for the H → D process is about 1.6 times higher than for the D → H process. In terms of the rate constant ratios shown in Table 3, this is due to the higher k_f/k_v ratio for the H → D process. The more fundamental reason for the higher H → D isotope exchange rate is, at this point, not evident. There are certainly important differences between reactive processes involving deuterium and hydrogen atoms. For example, due to the primary isotope effect, the activation energy for breaking a hydrogen bond is lower than that for breaking a similar deuterium bond. While such an isotope effect may be the reason for the higher γ_{o-p} observed in the H → D process, the present data do not lend themselves to an analysis in terms of such basic principles.

Models for Surface Uptake

To proceed further with the kinetic analysis of the surface uptake requires a molecular model of surface properties. The vapor−liquid interface of water is a sharp but finite transition, few molecular diameters thick within which density increases from the gas to the liquid. It can conveniently be described by a thickness, δ, on the order of 10^{-7} cm. To interpret α via eq 8 and resolve the surface kinetics expressed as ratios of rate coefficients in Table 3, absolute values of k_{sol} and k_{des} are needed. In our previous work we have formulated k_{sol} and α in terms of a critical cluster nucleation model, where uptake is controlled by aggregation of solvent (water) molecules around the incoming trace gas molecule within the interface.[2,37] Here we will present another independent approach, based on estimating surface concentration from Gibbs surface excess derived from the surface tension measurement of ethanol−water solutions. We examine the implications of these two interfacial formulations in terms of the kinetics presented in the last section. As will be evident, neither of these approaches gives an entirely satisfactory picture of interface—nor do recent numerical molecular dynamics simulations. The isotope exchange results imply an interfacial structure that is more complex than previously considered.

Surface Nucleation Model. This model assumes the interface is a dynamic region where aggregates are continually forming, falling apart, and re-forming. Nucleation theory, which describes the formation of a new phase, provides a viable description of such surface dynamics. In this context the formation of the new

TABLE 4: Kinetic Parameters for Ethanol Uptake Inferred by Estimating *K* via the Nucleation Model[a]

	273 K	283 K	291 K
$K = k_f/k_b$	0.041	0.032	0.025
k_{des} (s^{-1})	$(3.1 \pm 0.3) \times 10^{10}$	$(3.4 \pm 0.3) \times 10^{10}$	$(3.6 \pm 0.4) \times 10^{10}$
k_{sol} (s^{-1})	$(3.4 \pm 0.3) \times 10^{9}$	$(2.7 \pm 0.3) \times 10^{9}$	$(2.2 \pm 0.2) \times 10^{9}$
k_f (s^{-1})	$(7.5 \pm 1.3) \times 10^{9}$	$(9.2 \pm 1.1) \times 10^{9}$	$(7.3 \pm 0.9) \times 10^{9}$
k_E (s^{-1})	$(8.6 \pm 10.2) \times 10^{8}$	$(1.8 \pm 0.8) \times 10^{9}$	$(2.0 \pm 1.1) \times 10^{9}$
k_2 (s^{-1})	$(1.6 \pm 0.4) \times 10^{11}$	$(1.3 \pm 0.2) \times 10^{11}$	$(1.3 \pm 0.2) \times 10^{11}$
k_b (s^{-1})	$(1.8 \pm 0.3) \times 10^{11}$	$(2.9 \pm 0.3) \times 10^{11}$	$(2.9 \pm 0.4) \times 10^{11}$
k_C (M^{-1} s^{-1})	$(1.7 \pm 1.1) \times 10^{15}$	$(8.6 \pm 2.7) \times 10^{14}$	$(3.5 \pm 1.6) \times 10^{14}$
k_V (s^{-1})	$(3.2 \pm 0.9) \times 10^{10}$	$(3.5 \pm 0.6) \times 10^{10}$	$(3.7 \pm 0.9) \times 10^{10}$

[a] Error limits are one standard deviation.

phase can be thought of as the formation of a more liquidlike aggregate (or cluster) from the more loosely bound surface species.

The equilibrium density of surface clusters (aggregates) composed of N molecules is proportional to exp $(-\Delta G_N/RT)$ where ΔG_N is the molar free energy for the formation of a cluster with N molecules. Classical nucleation theory shows that ΔG_N first increases with cluster size, reaches a maximum, and then decreases. The initial resistance to cluster growth (formation of the new phase), is due to a surface free energy barrier associated with the phase boundary. The barrier is entropic in nature. The driving force is such that clusters smaller than a critical size (N^*) fall apart, whereas clusters larger than the critical size serve as centers for further condensation and grow in size until they merge into the adjacent bulk liquid.

The kinetics of critical cluster growth were expressed in terms of a surface state n_s and a weakly bound critical cluster state n_s^*, which are equivalent to n_w and n_p introduced in the previous section (see discussion following eq 20 and note 36). An incoming gas molecule such as ethanol, upon striking the surface, becomes a loosely bound surface species (n_w in eq 19), which participates in this nucleation process. If such a molecule becomes part of a critical sized cluster, it will be incorporated into the bulk liquid, at a rate k_2, via aggregation growth. The ethanol molecules aggregated into a critical cluster (i.e., n_s^* in ref 2) can be identified with the partially solvated species n_p in eq 19. Our measurements of α as a function of temperature yield values of the Gibbs energy (ΔG_{obs}) for this state. For ethanol the nucleation model yields a value of $N^* = 2.5$ (the average sum of trace gas and water molecules) required for further cluster growth and subsequent uptake into the liquid.

The nucleation model gives an estimate of the Gibbs energy (ΔG_w) of the weakly solvated state (n_w) that is about one-tenth of the species solvation energy, based on analysis of mass accommodation coefficients for over 20 species.[2] With this estimate, we can obtain the ratio $k_f/k_b = \exp[-(\Delta G_{obs} - \Delta G_w)/RT]$. This ratio together with the ratios in Table 3 and an estimate of the thickness of the interfacial region set at 10^{-7} cm, yields estimated rate constants listed in Table 4. Rate constants are shown only for the three temperatures where a full range of studies was performed. Of particular interest are the values of $k_{des} \sim 10^{10}$ s^{-1}, $k_{sol} \sim 10^9$ s^{-1}, and $k_c \sim 10^{15}$ M^{-1} s^{-1}, which can be compared to other gas/liquid kinetic formulations.

Gibb's Surface Excess Model. This model begins with the assumption that the equilibrium concentration of the surface species $n_s = (n_w + n_p)$ participating in the kinetics of the uptake process described by eq 19, is given by the Gibbs adsorption excess. This quantity, in turn, can be obtained from surface tension data by using the Gibbs adsorption equation.[38] At low surface coverages the number of ethanol molecules per unit area, n_s, is expected to be proportional to both the aqueous phase mole fraction, X_2, and the coverage, n_∞, corresponding to a complete monolayer; that is,

$$n_s = \beta X_2 n_\infty \tag{28}$$

where β is the dimensionless adsorption coefficient. The Gibbs adsorption equation provides the surface excess concentration rather than the total surface concentration; however, if β is much larger than unity, the two are essentially equal at low surface coverages. β is on the order of 80 for ethanol on water.

If we substitute eq 28 into the Gibbs adsorption equation, we obtain for the surface tension:

$$\sigma = \sigma_o - \beta X_2 n_\infty k_B T \tag{29}$$

where σ_o is the surface tension of pure water and k_B is Boltzmann's constant. n_∞ has a value of 4.9×10^{14} molecules cm^{-2}.[39]

This equation is strictly applicable only at very low concentrations where the surface adsorption behaves ideally. To our knowledge, surface tension data at the lowest ethanol concentration are those of Teitelbaum and co-workers, as tabulated by Timmermans.[40] These data extend down to $X_2 = 0.0018$; we have used the surface tensions at this concentration in eq 29 to estimate β as a function of temperature. The surface tension data show a pronounced change in slope above this concentration; as a result, our estimated values of β may be systematically in error. The temperature dependence of β, based on data from 0 to 40 °C, can be described by

$$\ln \beta = 3.14 + 370/T \tag{30}$$

To obtain an expression for the desorption rate k_{des}, we invoke detailed balance at the gas−liquid interface via $(\bar{c}/4)n_g = k_{des}n_s$ and express n_g in terms of the liquid-phase mole fraction via Henry's law coefficient as $n_g = X_2\rho N_A/(HRTM)$. Here, M is the molecular weight of water, ρ is the water density, and N_A is Avogadro's number. Then using eqs 28 and 30, with Henry's law coefficient as given by Snider and Dawson,[32] we obtain k_{des} (s^{-1}):

$$\ln(k_{des}) = 37.36 - 6864/T \tag{31}$$

This equation yields a lifetime toward desorption increasing from 0.19 μs at 40 °C to 4.8 μs at 0 °C.

To proceed further, we need to make some assumption about the equilibrium constant, K. For any given value of K, we can use eqs 24 and 25 to derive specific values of k_2, k_b, k_C, k_f, and k_E using the rate constant ratios obtained from the fits. As K approaches zero, k_f and k_E (the rate constants for the weakly adsorbed state) approach constant, minimum values while the other rate constants diverge toward infinity. As K approaches infinity, k_2, k_b, and k_C (the rate constants for the partially solvated state) approach constant, minimum values while the other rate

TABLE 5: Kinetic Parameters for Ethanol Uptake on Water Based on the Gibbs Surface Model[a]

		273 K	283 K	291 K
k_{des} (s^{-1})	$(2.1 \pm 0.3) \times 10^5$	$(5.0 \pm 0.7) \times 10^5$	$(9.7 \pm 1.5) \times 10^5$	
k_{sol} (s^{-1})	$(2.3 \pm 0.4) \times 10^4$	$(4.0 \pm 0.6) \times 10^4$	$(5.8 \pm 1.0) \times 10^4$	
		Lower Bounds		
k_f (s^{-1})	$(5.2 \pm 1.0) \times 10^4$	$(1.4 \pm 0.2) \times 10^5$	$(2.2 \pm 0.4) \times 10^5$	$K = 0$
k_E (s^{-1})	$(5.7 \pm 6.8) \times 10^3$	$(2.6 \pm 0.9) \times 10^4$	$(5.3 \pm 2.4) \times 10^4$	$K = 0$
k_2 (s^{-1})	$(4.7 \pm 1.1) \times 10^4$	$(6.2 \pm 1.0) \times 10^4$	$(9.7 \pm 1.8) \times 10^4$	$K = \infty$
k_b (s^{-1})	$(5.2 \pm 1.0) \times 10^4$	$(1.4 \pm 0.2) \times 10^5$	$(2.2 \pm 0.4) \times 10^5$	$K = \infty$
k_C (M^{-1} s^{-1})	$(5.0 \pm 2.6) \times 10^8$	$(4.8 \pm 1.2) \times 10^8$	$(3.0 \pm 1.2) \times 10^8$	$K = \infty$

[a] Error limits are one standard deviation. Lower bounds occur when either $K = 0$ or $K = \infty$, as indicated.

constants diverge. The minimum values obtained in these two limits are given in Table 5. The magnitudes of the rate constants do not change greatly between the assumed limit values for K. For example, when $K = 1$ each of the rate constants has a value equal to twice its minimum.

Comparison of the Surface Nucleation and Gibbs Surface Models. Tables 4 and 5 show that the two models provide significantly different pictures of gas uptake kinetics. In both models the ratio k_{sol}/k_{des} is about 0.1, since both were matched to the measured value of $\alpha \sim 0.1$. Likewise in both models k_{sol}/k_{des} exhibits a negative temperature dependence, matched to the observed variation of α with temperature. However, the derived values of k_{sol} and k_{des} differ by about 5 orders of magnitude, 10^8 $s^{-1}/10^9$ s^{-1} vs 10^4 $s^{-1}/10^5$ s^{-1} for the nucleation and surface excess models, respectively. This difference extends to the temperature dependence of k_{sol} and k_{des}. In the nucleation model k_{des} and k_{sol} have flat and negative temperature dependencies, respectively. The negative temperature dependence of k_{sol} reflects the energy of formation for the critical cluster in the nucleation model, indicating that increasing resistance to solvation (clustering) limits mass accommodation at increasing temperature. In the surface excess model, both k_{sol} and k_{des} have positive temperature dependencies, with an overall negative dependence of α arising from a stronger positive temperature dependence for k_{des}. The increasing value of k_{sol} with temperature is likely indicative of mass transport (i.e., diffusion) process.

In examining these models, the aim is to explain the nature of the barrier to mass accommodation inherent in the observation of $\alpha < 1$. In the development of the nucleation model for mass accommodation, transport effects were explicitly neglected by assuming that at the barrier (described as a critical cluster of trace gas and solvent molecules) transport was isotropic; i.e., there was no difference in the rates of diffusion into the bulk and of transport back across the interface into the gas phase. If, indeed, some of the barrier to accommodation is due to transport resistance, then the nucleation model parameters would likely be adjusted in the direction of transport process kinetics implied by the surface excess model.

The interfacial kinetic parameters in Tables 4 and 5 can be compared to other relevant kinetic rates. For example, the surface excess model yields a low value for the solvation rate k_{sol}. This can be demonstrated by setting up the equilibrium condition between the Gibbs surface and the bulk phase. With k_{-2} defined as the transport rate from bulk to surface we obtain $\beta k_{sol} = k_{-2}$. The thickness (δ) of the transition region from the Gibbs surface to the bulk phase is likely to be on the order 10^{-7} cm. The rate k_{-2} is expected to be the inverse of the transport time across the transition region. That is, $k_{-2} \sim D_l/\delta^2$. The liquid-phase diffusion coefficient D_l is about 10^{-5} cm^2 s^{-1}; therefore k_{-2} is on the order 10^9 s^{-1}. The coefficient β for ethanol is about 10^2, yielding $k_{sol} \sim 10^7$ s^{-1}, which is about 3 orders of magnitude faster than obtained from the surface excess model in Table 5. Such a low apparent diffusion rate would appear to represent a physically unrealistic barrier to transport.

On the other hand, the value of 10^{15} M^{-1} s^{-1} derived from the nucleation model for the acid/base-catalyzed isotope exchange rate constant, k_c, is unrealistically high. The rate constant for this process in bulk solution for methanol in water is reported to be 6×10^8 M^{-1} s^{-1}.[35] While on a surface the reaction may proceed faster than in the bulk, a value of 10^{15} M^{-1} s^{-1} is not likely to be attained and is several orders of magnitude too high. By contrast, the lower limit values of k_c in the region 5×10^8 M^{-1} s^{-1} obtained from the Gibbs surface model, are certainly reasonable. The implication of these kinetic considerations is that rates derived from the nucleation model are unreasonably fast while some of the rates obtained from the surface excess model are too slow.

Another point of comparison involves the surface concentration, n_s. The 10^5 difference in k_{des} values for the two models corresponds to a 10^5 difference in n_s. For the nucleation model, which is based on an assumed accommodation mechanism and does not make any direct assumptions about surface concentrations, the derived n_s might be significantly increased with inclusion of transport effects in the mechanism, as discussed above. The central difference between the two models is that the nucleation model does not explicitly treat n_s (the values in Table 4 are estimated only by kinetic balance for an interfacial thickness $\delta = 10^{-7}$ cm), while the surface excess model starts with a value for n_s derived from surface tension measurements. The key question is the validity of the assumption that the Gibbs surface excess derived from β (eq 28) can be equated with n_s in eqs 5 and 20.

The isotope exchange results lead to the use of a complex interfacial model that differentiates the surface species n_s into weakly bound (n_w) and partially solvated (n_p) components, analogous to the nucleation model of mass accommodation.[2] Although the kinetic results lack sufficient information to determine the weighting of n_w and n_p, the implications of the two surface models can be compared in terms of the position of the uptake barrier relative to the Gibbs surface. The Gibbs surface model suggests that the uptake barrier must be near the position of the ion solvation barrier, which is within the Gibbs surface.[33] On the other hand, the nucleation model, in which the derived reactive surface density is much lower than the Gibbs surface excess, predicts the position of the barrier to be at the outer (near the gas) edge of the Gibbs surface. Reactions with ions at such a distance from the ion solvation barrier are presumably possible because the water cluster around the ethanol forms an aqueous path around the ions. As noted above, the nucleation model explicitly ignores any possible transport resistance associated with such a process, perhaps accounting for the quantitative discrepancy in the two approaches. The overall point is that an average critical cluster size of 2.5, derived

for EtOH accommodation, is about equal to the thickness of the ion solvation barrier.

Conclusions

For both acetic acid and ethanol we have reproduced our earlier uptake measurements and have shown that the isotope exchange process at the interface further increases the species uptake (loss). These results confirm our previous studies, which indicate that mass accommodation coefficients for trace gases on liquid water are in general less than unity, leading to the conclusion that there is a significant interfacial barrier to uptake from the gas into the liquid. The results of the isotope exchange studies led to the formulation of a kinetic model in which it is assumed that the surface adsorbed ethanol molecules are distributed between two distinct forms; a weakly adsorbed state, and a partially solvated state. Only the partially solvated molecules can interact with the near-surface ions in the interior of the liquid. The kinetics is further examined using two models to describe the surface species: surface nucleation and Gibbs surface excess.

As stated earlier, molecular dynamics simulations of ethanol uptake by water, recently performed by Taylor et al.[3] and Wilson and Pohorille,[4] yield a value for the mass accommodation coefficient of essentially unity. The much lower experimental values imply that the simulations do not simulate the resistance to the transfer of a molecule from the gas to the liquid. This resistance could be due to two factors. It could be in the form of a free energy maximum caused by the necessary initial rearrangement of molecules on the way to solvation, or it could be due to a minimum in the surface to bulk diffusion coefficient (or some combination of the two). The nucleation model suggests that the barrier is due to a maximum in free energy. The Gibbs surface model suggests that the barrier is due to a lower diffusion rate. At this point, none of these models provides a satisfactory description of the uptake process within the complex structure of the vapor/water interface implied by the EtOH isotope exchange results. Further work, both on gas uptake and on the structure of the interface, will be necessary to clarify these issues.

Acknowledgment. Funding for this work was provided by the National Science Foundation Grant No. ATM-96-32599, the U.S. Environmental Protection Agency Grant No. R-821256-01-0, and Department of Energy Grant Nos. DE-FG02-91ER61208 and DE-FG 02-98ER62581. We thank Professors S. J. Miller and L. T. Scott for helpful discussions. The authors would also like to thank Dr. Thomas Peter whose thoughtful comments made an important contribution to this publication.

References and Notes

(1) Kolb, C. E.; Worsnop, D. R.; Zahniser, M. S.; Davidovits, P.; Keyser, L. F.; Leu, M.-T.; Molina, M. J.; Hanson, D. R.; Ravishankara, A. R.; Williams, L. R.; Tolbert, M. A. Laboratory studies of atmospheric heterogeneous chemistry. In *Progress and Problems in Atmospheric Chemistry*; Barker, J. R., Ed.; Advanced Series in Physical Chemistry 3: World Scientific: Singapore, 1995; pp 771−875.

(2) Nathanson, G. M.; Davidovits, P.; Worsnop, D. R.; Kolb, C. E. *J. Phys. Chem.* **1996**, *100*, 13007.

(3) Taylor, R. S.; Ray, D.; Garrett, B. C. *J. Phys. Chem. B* **1997**, *101*, 5473.

(4) Wilson, M. A.; Pohorille, A. *J. Phys. Chem. B* **1997**, *101*, 3130.

(5) Rouhi, A. M. *Chem. Eng. News* **1997**, December 21, 38.

(6) Govoni, S. T.; Nathanson, G. M. *J. Am. Chem. Soc.* **1994**, *116*, 779.

(7) Klassen, J. K.; Nathanson, G. M. *Science* **1996**, *273*, 333.

(8) Klassen, J. K.; Fiehrer, K. M.; Nathanson, G. M. *J. Phys. Chem. B* **1997**, *101*, 9098.

(9) Hanson, D. R.; Ravishankara, A. R. *J. Phys. Chem.* **1994**, *98*, 5728.

(10) Hanson, D. R. *J. Phys. Chem.* **1998**, *102*, 4794.

(11) Hu, J. H.; Shi, Q.; Davidovits, P.; Worsnop, D. R.; Zahniser, M. S.; Kolb, C. E. *J. Phys. Chem.* **1995**, *99*, 8768.

(12) George, C.; Behnke, W.; Scheer, V.; Zetzsch, C.; Magi, L.; Ponche, J. L.; Mirabel, Ph. *Geophys. Res. Lett.* **1995**, *22*, 1505.

(13) Worsnop, D. R.; Zahniser, M. S.; Kolb, C. E.; Gardner, J. A.; Watson, L. R.; Van Doren, J. M.; Jayne, J. T.; Davidovits, P. *J. Phys. Chem.* **1989**, *93*, 1159.

(14) Jayne, J. T.; Worsnop, D. R.; Kolb, C. E.; Swartz, E.; Davidovits, P. *J. Phys. Chem.* **1996**, *100*, 8015.

(15) Robinson, G. N.; Worsnop, D. R.; Jayne, J. T.; Kolb, C. E.; Davidovits, P. *J. Geophys. Res.* **1997**, *103*, 3583.

(16) Jayne, J. T.; Duan, S. X.; Davidovits, P.; Worsnop, D. R.; Zahniser, M. S.; Kolb, C. E. *J. Phys. Chem.* **1991**, *95*, 6329.

(17) Mozurkewich, M. *Aerosol Sci. Technol.* **1986**, *5*, 223.

(18) Danckwerts, P. V. *Trans. Faraday Soc.* **1951**, *47*, 1014.

(19) Danckwerts, P. V. *Gas−Liquid Reactions*; McGraw-Hill: New York, 1970.

(20) Crank, J. *Mathematics of Diffusion*; Oxford University Press: Amen House, London, E.C.4, 1956.

(21) Robinson, G. N.; Worsnop, D. R.; Jayne, J. T.; Kolb, C. E.; Swartz, E.; Davidovits, P. *J. Geophys. Res.* in press.

(22) Houghton, G. *J. Chem. Phys.* **1964**, *40* (4), 1628.

(23) Fuchs, N. A.; Sutugin, A. G. *Highly dispersed aerosols;* Ann Arbor Science: Ann Arbor, MI, 1970.

(24) Widmann, J. F.; Davis, E. J. *J. Aerosol Sci.* **1997**, *28*, 87.

(25) Hanson, D. R.; Ravishankara, A. R.; Lovejoy, E. R. *J. Geophys. Res.* **1996**, *101*, 9063.

(26) In our earlier work, gas-phase diffusion was taken into account via the expression (ref 13) $1/\Gamma_{diff} = \bar{c}d_f/8D_g - 1/2$. This simpler formulation is in agreement with eq 13 to better than 5% in the range of *Kn* (0.1 and 1) and γ_o less than 0.3 applicable to our earlier studies. The difference between γ_o obtained with the two formulations increases with increasing γ_o and decreasing *Kn*.

(27) Swartz, E.; Shi, Q.; Davidovits, P.; Jayne, J. T.; Worsnop, D. R.; Kolb, C. E. *J. Phys. Chem.*, submitted.

(28) Key, R. J.; Dixon-Lewis, G.; Warnatz, J.; Coltrin, M. E.; Miller, J. A. Report SAN086-8256; Sandia National Laboratory: Albuquerque, NM, 1986.

(29) Formally, the absence of evaporation (and thus time independence of uptake) is taken into account by adding a bulk reaction channel to the uptake formulation. This is done by replacing the term Γ_{sol} with the sum $\Gamma_{sol} + \Gamma_{rxn}$ in eqs 4 and 10. The Γ_{rxn} term accounts for diffusion-limited reaction in the bulk liquid below the interface. Note that Γ_{rxn} is time independent and depends on the square root of the reaction rate (and therefore reactant concentration). (See ref 11.) In the limit of a fast reaction, $\Gamma_{rxn} \gg \Gamma_{sol}$, resulting in time independent uptake. This appears to be the case for deuterated ethanol isotope exchange in the bulk water.

(30) Hanson, D. R. *J. Phys. Chem.* **1997**, *101*, 4998.

(31) Note that eq 2 in ref 13 is equivalent to eq 17 for a droplet train of fixed frequency. In that case, droplet surface area is varied by switching the droplet train on and off, so that n_g and n_g' are the gas concentrations at the inlet and outlet of the flow tube. When using the frequency switching technique, which avoids problems associated with blocking the droplet stream, the gas concentration at the inlet of the flow tube is not measured. It can easily be shown that eq 17, which includes ΔA derived from different droplet driving frequencies, is equivalent to eq 2 in ref 13 with n_g and n_g' representing the trace gas concentration at the outlet of the flow tube as noted in the text here.

(32) Snider, J. R.; Dawson, G. A. *J. Geophys. Res.* **1985**, *90*, 3797.

(33) Benjamin, I. *Chem. Rev.* **1996**, *96*, 1449.

(34) Luz, Z.; Gill, D.; Meiboom, S. *J. Chem. Phys.* **1959**, *30*, 1540.

(35) Hills, B. P. *J. Chem. Soc., Faraday Trans.* **1990**, *86*, 481.

(36) Note that in ref 2, n_s was defined as a concentration with units (molecules cm^{-3}). Thus, the surface density n_s defined here with units (molecules cm^{-2}) is actually equivalent to $n_s\delta$ in ref 2 where δ is an assumed thickness of the interface. Also, in ref 2, k_b was omitted for simplicity, since it drops out of the final formulation of α (see eq 8) if n_s and n_s* are not experimentally distinguishable.

(37) Davidovits, P.; Jayne, J. T.; Duan, S. X.; Worsnop, D. R.; Zahniser, M. S.; Kolb, C. E. *J. Phys. Chem.* **1991**, *95*, 6337.

(38) Lewis, G. N.; Randall, M.; Pitzer, K. S.; Brewer, L. *Thermodynamics*, 2nd ed.; McGraw-Hill: New York, 1961.

(39) Butler, J. A. V.; Wightman, A. *J. Chem. Soc.* **1932**, 2089.

(40) Timmermans, J. *The Physicochemical Constants of Binary Systems in Concentrated Solutions;* Interscience: New York, 1960; Vol. 4.